Kinetic and Thermodynamic Studies of Thermal Dehydration of the Synthetic Magnesium Orthophosphate Octahydrate

การศึกษาจลนพลศาสตร์และอุณหพลศาสตร์การขจัดน้ำเชิงความร้อนของสารสังเคราะห์แมกนีเซียมออร์โธฟอสเฟตออกตะไฮเดรต

Nantawat Phonchan (นันทวัท ผลจันทร์)* Dr.Chanaiporn Danvirutai (ดร.ไฉนพร ด่านวิรุทัย)**
Dr.Tipaporn Sritharatana (ดร.ทิพาภรณ์ ศรีธัญรัตน์) ***

ABSTRACT

Thermal dehydration kinetics of the synthetic $Mg_3(PO_4)_2\cdot 8H_2O$ was studied by using thermogravimetric/ differential thermogravimetric/ differential thermal analysis (TG/DTG/DTA) techniques at four heating rates. The activation energy values were calculated by using Ozawa and Kissinger equations. The calculated activation energy values from both methods are close to each other. The most probable mechanism function with the integral form of $g(\alpha) = -\ln(1-\alpha)$ and the differential form $f(\alpha) = (1-\alpha)$ can be suggested to be the mechanism function of the 1st step while the most probable mechanism function of 2nd step cannot be determined. The thermodynamic functions of the transition state complexes were estimated by Eyring method. The positive values of $\Delta H^{\neq}$ and $\Delta G^{\neq}$ indicated that the dehydration is an endothermic process and is a non-spontaneous process.

บทคัดย่อ

ได้ศึกษาจลนพลศาสตร์การขจัดน้ำเชิงความร้อนของแมกนีเซียมฟอสเฟตออกตะไฮเดรตที่สังเคราะห์ขึ้นโดยใช้ข้อมูลจากเทคนิคเทอร์มอกราวิเมตริก/ ดิฟเฟอเรนเชียลเทอร์มอกราวิเมตริก/ ดิฟเฟอเรนเชียลเทอร์มาลอะนาไลซิส (TG/DTG/DTA) ณ อัตราการเพิ่มอุณหภูมิ 4 อัตรา คำนวณพลังงานกระตุ้นด้วยสมการของ Ozawa และ KAS พบว่าพลังงานกระตุ้นจากทั้ง 2 วิธีมีค่าใกล้เคียงกัน ฟังก์ชันของกลไกที่เหมาะสมสำหรับการขจัดน้ำในขั้นตอนแรกมีรูปอินทิกรัลคือ $g(\alpha) = -\ln(1-\alpha)$ และมีรูปอนุพันธ์คือ $f(\alpha) = (1-\alpha)$ ในขณะที่การขจัดน้ำในขั้นตอนที่ 2 นั้นไม่สามารถหาฟังก์ของกลไกที่เหมาะสมได้ ใช้ระเบียบวิธีของ Eyring ในการในการประมาณค่าฟังก์ชันทางอุณหพลศาสตร์ของสถานะกระตุ้นเชิงซ้อนพบว่าการเปลี่ยนแปลงเอนทาลปีและพลังงานอิสระของกิบบส์มีค่าเป็นบวก แสดงให้เห็นว่าการขจัดน้ำของสารที่ศึกษาเป็นกระบวนการดูดความร้อนและเป็นกระบวนการที่ไม่สามารถเกิดได้เอง

Key Words: Magnesium phosphate, Thermal decomposition kinetics, Thermodynamic functions

คำสำคัญ: แมกนีเซียมฟอสเฟต จลนพลศาสตร์การสลายตัวเชิงความร้อน ฟังก์ชันทางอุณหพลศาสตร์

** Master degree student, Center of Excellence for Innovation in Chemistry (PERCH-CIC), Department of Chemistry, Faculty of Science, Khon Kaen University*

*** Asst. Prof. Center of Excellence for Innovation in Chemistry (PERCH-CIC), Department of Chemistry, Faculty of Science, Khon Kaen University*

**** Asst. Prof. Department of Chemistry, Faculty of Science, Khon Kaen University*

Introduction

$Mg_3(PO_4)_2{\cdot}8H_2O$ and its final decomposition product, $Mg_3(PO_4)_2$ are of great interest nowadays. They are widely used in several fields such as agricultural, pharmaceutical, food and textile industry because of they are the absence of ecologically (toxicology) harmful elements (Mesíková, Śulková & Trojan, 2007). Main properties of magnesium phosphate are insolubility in water, temperature resistance and chemical stability. Therefore, it can be used as an anticorrosive pigment (Aramendía, Borau, Jiménez, Marinas & Romero, 1999a). Furthermore, $Mg_3(PO_4)_2$ exhibits the property as catalysts for various organic reactions such as the production of 1-hexene and 2-hexene from the dehydration of 2-hexanol (Aramendía et al., 1999a), N-alkylation of aniline with methanol (Aramendía, Borau, Jiménez, Marinas & Romero, 1999b) and the oxidative dehydrogenation of ethane (Sugiyama, Kondo, Satomi, Hayashi & Moffat, 1995). The kinetic and thermodynamic studies of solid-state reactions are remarkable for decades due to the thermal stability, decomposition rate and life time prediction of materials and systems under different experimental and environmental conditions can be provided. In previous works, thermal decomposition kinetics and some of thermodynamic functions of some metal hypophosphite monohydrate and metal phosphate hydrates were studied (Noisong, Danvirutai & Boonchom, 2009; Boonchom & Danvirutai, 2009; Danvirutai, Noisong & Youngme, 2008).

In this work, the purpose is to study the kinetic and thermodynamic properties of the thermal dehydration of the synthetic $Mg_3(PO_4)_2{\cdot}8H_2O$ by using TG/DTG/DTA data. Non-isothermal dehydration kinetics was carried out by using Ozawa and Kissinger-Akahira-Sunose (KAS) equations. The thermodynamic functions ($\Delta S^{\neq}$, $\Delta H^{\neq}$, $\Delta G^{\neq}$) were estimated by using the transition state complexes theory of Eyring (Rooney, 1995). All parameters from Ozawa and KAS methods are compared and discussed.

Materials and Methods

Synthesis and Characterization

$Mg_3(PO_4)_2{\cdot}8H_2O$ samples were synthesized by precipitation method using 0.50 M $Mg(NO_3)_2{\cdot}6H_2O$ and 0.10 M $Na_3PO_4{\cdot}12H_2O$ in the desired molar ratio of Mg:P. The white suspension of product was stirred for 24 h at room temperature, filtered by suction pump, washed three times with de-ionized water and dried in a desiccator for overnight. The synthesized samples and its calcined product at 750 °C were characterized by X-ray powder diffraction (XRD, Phillips 3710), Fourier transform infrared (FTIR) spectroscopy (Perkin Elmer Spectrum GX), thermogravimetric/ differential thermogravimetric/ differential thermal analysis in nitrogen atmosphere (TG/DTG/DTA, Perkin Elmer Pyris Diamond), and atomic absorption spectrophotometry (AAS, Perkin Elmer Analyst 100).

Kinetic Study

Dehydration and decomposition of crystalline hydrates is a solid-state process of the type: A(solid) $\longrightarrow$ B(solid) + C(gas) (Vlase, T., Vlase, G., Daca, M. & Doca, N., 2003). The kinetics of such reactions is described by various equations taking into account the special features of their mechanisms. All kinetic studies are assumed to be based on the following equations:

$$\frac{d\alpha}{dt} = kf(\alpha) \tag{1}$$

and

$$k = Ae^{-E_\alpha / RT} \tag{2}$$

where α is the extent of conversion and is equal to $(m_0 - m_t)/(m_0 - m_f)$; m_0, m_t, and m_f are the initial mass of sample, current mass of sample at temperature t, and final mass at a temperature at which the mass loss is approximately unchanged, respectively. *f(α)* is a function depending on the particular decomposition mechanism and is referred to as the difficult form. The pre-exponential factor, *A* (min^{-1}) is assumed to be independent of temperature, E_α is the activation energy (kJ mol^{-1}), *R* is the gas constant (8.314 J K^{-1} mol^{-1}), and *k* is the rate constant. Combination of eqs. (1) and (2) gives

$$\frac{d\alpha}{dt} = Af(\alpha)e^{-E_\alpha/RT} \tag{3}$$

Eq (3) can be modified, when β is the heating rate (β = dT/dt), T is temperature (K), and t is time, and the following equation is obtained:

$$\frac{d\alpha}{dt} = \frac{dT}{dt}\frac{d\alpha}{dT} = \beta\frac{d\alpha}{dT} = Af(\alpha)e^{-E_\alpha/RT} \tag{4}$$

Eq (4) can be rearranged to eq (5) as follows:

$$\frac{d\alpha}{f(\alpha)} = \frac{A}{\beta}e^{-E_\alpha/RT}dt \tag{5}$$

The solution of the left-hand side integral depends on the explicit expression of the function *f(α)* and is denoted as *g(α)*. Various scientists suggested different ways to solve the right-hand side of eq (5). Thus, the kinetics of solid-state reactions can be described by various equations taking into account the special features of their mechanism. In kinetic study of $Mg_3(PO_4)_2{\cdot}8H_2O$, Ozawa and KAS equations were used to determine the activation energy (E_α) and pre-exponential factor (*A*) of the dehydration reaction. These methods are well described and widely used in the literatures, which provides reliable results. Therefore, these methods are selected for kinetic analysis of the dehydration of the studied compound. The equations used for E_α calculation are

Ozawa equation (Ozawa, 1965):

$$\ln\beta = \ln\left(\frac{0.0048AE_\alpha}{g(\alpha)R}\right) - 1.0516\left(\frac{E_\alpha}{RT}\right) \tag{6}$$

KAS equation (Kissinger, 1957; Akahira & Sunose, 1971):

$$\ln\left(\frac{\beta}{T^2}\right) = \ln\frac{AR}{g(\alpha)E_\alpha} - \frac{E_\alpha}{RT} \tag{7}$$

All other parameters are the same as given in eqs. (1) and (2). The Arrhenius parameters, together with the reaction model, are sometimes called the kinetic triplet. *g(α)* is the integral form of *f(α)*, which is the reaction model that depends on the reaction mechanism. According to the above-mentioned equations, the plots of lnβ versus 1000/*T* (eq. (6)) and $\ln(\beta/T^2)$ versus 1000/*T* (eq. (7)) corresponding to different extents of conversion α can be obtained by a linear regression of the least-squares method. The activation energy E_α and pre-exponential factor *A* can be evaluated from the slopes and intercept of the straight lines with better linear correlation coefficients (r^2), respectively. The activation energy values were calculated at the heating rates of 5, 10, 15, and 20 °C min^{-1} via the mentioned methods in the α range of 0.2–0.8.

Determination of the Most Probable Mechanism Function and Pre-exponential Factor

Some of kinetic results in the literature showed that the kinetic parameters depend on the selection of a proper mechanism function for the process (Vlaev, Nedelchev, Gyurova & Zagorcheva, 2008). In this present work, the most probable mechanism function can be determined by using the equations as stated in Table 1.

Table 1 All 26 types of mechanism functions *g(α)* and *f(α)* used for the present analysis

No.	Symbol	Mechanism function name	*f(α)*	*g(α)*
1.	$F_{1/3}$	one-third order	$3/2(1 - \alpha)^{1/3}$	$1 - (1 - \alpha)^{2/3}$
2.	$F_{3/4}$	three-quarters order	$4(1 - \alpha)^{3/4}$	$1 - (1 - \alpha)^{1/4}$
3.	$F_{3/2}$	one and a half order	$2(1 - \alpha)^{3/2}$	$(1 - \alpha)^{-1/2} - 1$
4.	F_2	second order	$(1 - \alpha)^2$	$(1 - \alpha)^{-1} -1$
5.	F_3	third order	$1/2(1 - \alpha)^3$	$(1 - \alpha)^{-2} - 1$
6.	$P_{3/2}$	Mampel power law	$(2/3)\alpha^{-1/2}$	$\alpha^{3/2}$
7.	$P_{1/2}$	Mampel power law	$2\alpha^{1/2}$	$\alpha^{1/2}$
8.	$P_{1/3}$	Mampel power law	$3\alpha^{2/3}$	$\alpha^{1/3}$
9.	$P_{1/4}$	Mampel power law	$4\alpha^{3/4}$	$\alpha^{1/4}$
10.	E_1	exponential law	α	$\ln\alpha$
11.	A_1, F_1	Arami-Erofeev equation	$(1 - \alpha)$	$-\ln(1 - \alpha)$
12.	$A_{3/2}$	Arami-Erofeev equation	$3/2(1 - \alpha)[-\ln(1 - \alpha)]^{1/3}$	$[-\ln(1 - \alpha)]^{2/3}$
13.	A_2	Arami-Erofeev equation	$2(1 - \alpha)[-\ln(1 - \alpha)]^{1/2}$	$[-\ln(1 - \alpha)]^{1/2}$
14.	A_3	Arami-Erofeev equation	$3(1 - \alpha)[-\ln(1 - \alpha)]^{2/3}$	$[-\ln(1 - \alpha)]^{1/3}$
15.	A_4	Arami-Erofeev equation	$4(1 - \alpha)[-\ln(1 - \alpha)]^{3/4}$	$[-\ln(1 - \alpha)]^{1/4}$
16.	R_1, F_0, P_1	power law	$(1 - \alpha)^0$	α
17.	R_2, $F_{1/2}$,	power law	$2(1 - \alpha)^{1/2}$	$1 - (1 - \alpha)^{1/2}$
18.	R_3, $F_{2/3}$	power law	$3(1 - \alpha)^{2/3}$	$1 - (1 - \alpha)^{1/3}$
19.	D_1	parabola law	$1/2\alpha$	α^2
20.	D_2	Valensi equation	$[-\ln(1 - \alpha)]^{-1}$	$\alpha + (1 - \alpha) \ln(1 - \alpha)$
21.	D_3	Jander equation	$3/2(1 - \alpha)^{2/3}[1 - (1 - \alpha)^{1/3}]^{-1}$	$[1 - (1 - \alpha)^{1/3}]^2$
22.	D_4	Ginstling-Brounstein equation	$3/2[(1 - \alpha)^{-1/3} - 1]^{-1}$	$1 - 2\alpha/3 - (1 - \alpha)^{2/3}$
23.	D_5	Zhuravlev, Lesokin, Tempelman equation	$3/2(1 - \alpha)^{4/3}[1 - \alpha)^{-1/3} - 1]^{-1}$	$[(1 - \alpha)^{-1/3} - 1]^2$
24.	D_6	anti-Jander equation	$3/2(1 + \alpha)^{2/3}[(1 + \alpha)^{1/3} - 1]^{-1}$	$[(1 + \alpha)^{1/3} - 1]^2$
25.	D_7	anti-Ginstling-Brounstein equation	$3/2[(1 + \alpha)^{-1/3} - 1]^{-1}$	$1 + 2\alpha/3 - (1 + \alpha)^{2/3}$
26.	D_8	anti-Zhuravlev, Lesokin, Tempelman equation	$3/2(1 + \alpha)^{4/3}[(1 + \alpha)^{-1/3} - 1]^{-1}$	$[(1 + \alpha)^{-1/3} - 1]^2$

$$\ln g(\alpha) = \left[\ln\frac{AE_\alpha}{R} + \ln\frac{e^{-x}}{x^2} + \ln h(x) \right] - \ln\beta \qquad (8)$$

where, x is E_α/RT and

$$h(x) = \frac{x^4 + 18x^3 + 88x^2 + 96x}{x^4 + 20x^3 + 120x^2 + 240x + 120}$$

which is expressed by the fourth Senum and Yang approximation (Senum and Yang, 1977). The plots of ln*g(α)* versus ln*β* were carried out by using a linear regression of the least-squares method. To determine the most probable mechanism function, the degrees of conversion *α* corresponding to four heating rates taken at the same temperature (we selected at 150 and 155 °C for the 1st step, and 210 and 220 °C at the 2nd step) were substituted into the left side of eq. (8) for all 26 types of mechanism functions as presented in Table 1 (Noisong and Danvirutai 2010). If the mechanism functions according to eq. (9) exhibits the slope and the linear correlation coefficient r^2 close to -1.0000 and unity, respectively, then the function *g(α)* is the most probable mechanism function. The results of the most probable mechanism functions during the dehydration process are tabulated in Table 2.

Estimation of Thermodynamic Functions of the Transition State Complexes

From the activated complexes (transition state) theory of Eyring, the following general equation may be written:

$$A = \left(\frac{e\chi k_B T_p}{h}\right)\exp\left(\frac{\Delta S^{\neq}}{R}\right) \qquad (9)$$

where A is the pre-exponential factor, $e = 2.7183$ is the Neper number, χ is the transition factor which is unity for the monomolecular reactions, k_B is the Boltzmann constant (1.3806×10^{-23} J K^{-1}), h is Planck's constant (6.6260×10^{-34} J s), and T_p is the average phase transformation temperature peak in DTG or DTA curves (K). The entropy change can be calculated according to the formula:

$$\Delta S^{\neq} = R\ln\left(\frac{Ah}{e\chi k_B T_P}\right) \qquad (10)$$

Since

$$\Delta H^{\neq} = E^{\neq} - RT_P \qquad (11)$$

$$\Delta G^{\neq} = \Delta H^{\neq} - T_P \Delta S^{\neq} \qquad (12)$$

when $E^{\neq}$ is the activation energy E_α calculated from TG/DTG/DTA data by using Ozawa and KAS equations. The enthalpy and Gibbs free energy changes ($\Delta H^{\neq}$ and $\Delta G^{\neq}$) for the activated complex formation from the reactant can be calculated using the well-known thermodynamic equations.

Results and Discussion

Characterization

The TG, DTG and DTA curves of the synthesized compound at four heating rates are illustrated in Fig. 1.

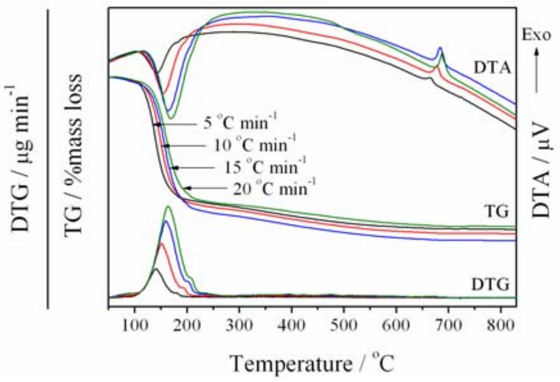

Figure 1 TG/DTG/DTA curves of the synthesized $Mg_3(PO_4)_2 \cdot 8H_2O$ at the heating rates of 5, 10, 15 and 20 °C min^{-1}

All curves are approximately in the same shape and indicate that the maximum temperature and the mass loss increase when increasing the heating rate. The observed total mass loss at the heating rate of 10 °C min^{-1} in the temperature range of 50 – 700 °C was found to be 26.15% (5.91 mole H_2O) and 7.56% (1.71 mole H_2O), which agree well with the theoretical value of $Mg_3(PO_4)_2 \cdot 8H_2O$ (35.42%, 8.00 mole H_2O). The retaining mass of about 66.29% is compatible with the value expected for the formation of $Mg_3(PO_4)_2$ which can be identified by XRD and FTIR techniques. Therefore, the suggested reactions of the dehydration are:

$$Mg_3(PO_4)_2 \cdot 8H_2O \longrightarrow Mg_3(PO_4)_2 \cdot 2H_2O + {\sim}6H_2O \qquad (13)$$

$$Mg_3(PO_4)_2 \cdot 2H_2O \longrightarrow Mg_3(PO_4)_2 + {\sim}2H_2O \qquad (14)$$

The mass loss is approximately unchanged at about 700 °C, therefore, the calcined temperature was observed and the final decomposition product, $Mg_3(PO_4)_2$ can be obtained.

The XRD patterns of the synthesized sample and its calcined product at 750 °C are shown in Fig. 2(a) and (b), respectively. All detectable peaks of the prepared sample are indexed to be $Mg_3(PO_4)_2 \cdot 8H_2O$ with the PDF standard file number 84–1147 while the detectable peaks of its calcined product at 750 °C are indexed to be $Mg_3(PO_4)_2$ using the standard PDF file number 33–0876 (Aramendía et al., 1999a).

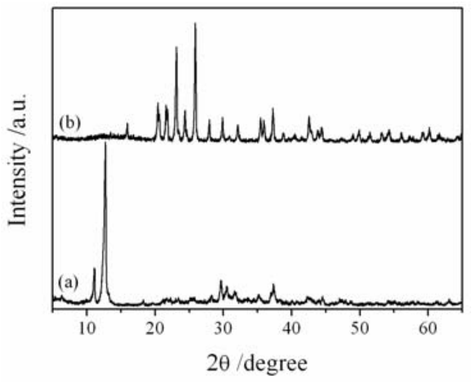

Figure 2 XRD patterns of the synthesized $Mg_3(PO_4)_2{\cdot}8H_2O$ (a) and its calcined product at 750 °C (b)

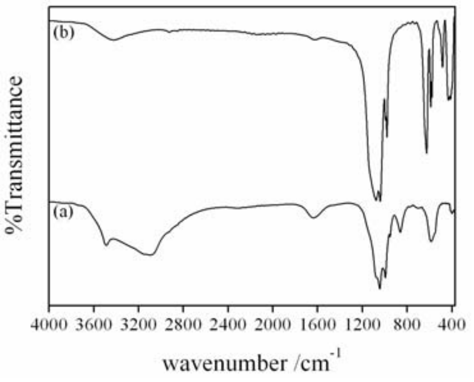

Figure 3 FTIR spectra of the synthesized $Mg_3(PO_4)_2{\cdot}8H_2O$ (a) and its calcined product at 750 °C (b)

The FTIR spectra of the as-prepared $Mg_3(PO_4)_2{\cdot}8H_2O$ and its calcined product at 750 °C are illustrated in Fig. 3. The FTIR spectrum of the synthesized sample in Fig. 3(a) is similar to the recorded spectrum of the commercially obtained $Mg_3(PO_4)_2{\cdot}8H_2O$ (Fluka) (Tabtimsai 2007). Two vibrational bands at 3153 and 3098 cm^{-1} are assigned to be $\nu_1(A_1)H_2O$, whereas the band at 3489 cm^{-1} is assigned to $\nu_3(B_2)H_2O$. The band at 1638 cm^{-1} corresponds to $\nu_2(A_1)H_2O$. Two bands at 954 and 995 cm^{-1} are attributed to $\nu_1(A_1)PO_4^{3-}$, while two bands at 1045 and 1075 cm^{-1} are attributed to $\nu_3(F_2)PO_4^{3-}$. The band at 399 cm^{-1} corresponds to $\nu_2(E)PO_4^{3-}$, while two bands at 554 and 587 cm^{-1} are attributed to the splitting of the triply degenerate mode $\nu_4(F_2)PO_4^{3-}$. One band at 862 cm^{-1} disappears in the spectrum of calcined product, which could be assigned to the H_2O libration. The observed bands at 982 and 995 cm^{-1} of the calcined product at 750 °C in Fig. 3(b) can be assigned to $\nu_1(A_1)PO_4^{3-}$, while three bands at 1042, 1078 and 1093 cm^{-1} are attributed to the complete splitting of the triply degenerate mode $\nu_3(F_2)PO_4^{3-}$ caused by the symmetry lowering from T_d. Four bands in the region of 486–399 and 626–578 cm^{-1} are assigned to $\nu_2(E)PO_4^{3-}$ and $\nu_4(F_2)PO_4^{3-}$, respectively. The splitting of the triply degenerate $\nu_4(F_2)$ and the doubly degenerate $\nu_2(E)$ bands either in hydrate and the calcined product indicate that the symmetry of the phosphate group is decreased from T_d symmetry to the lower one.

The magnesium content of the synthesized sample from AAS method was found to be 16.33% (2.73 mole Mg), which agrees with the calculated value of 17.92% (3.00 mole Mg for $Mg_3(PO_4)_2{\cdot}8H_2O$).

Calculation of Activation Energy Values, Determination of the Most Probable Mechanism Function and Pre-exponential Factors

The calculated results from Ozawa and KAS methods according to four TG measurements are presented in Fig. 4 – 7. The activation energy values E_a for the 1st step and the 2nd step are tabulated in Table 2 and 3, respectively. The average activation energy values from the conversion factor from 0.2 to 0.8 of

Ozawa and KAS methods for the 1st step are 91.67 and 89.40 kJ mol^{-1}, respectively. The activation energy of the 1st step of dehydration is reliable via the very small difference of the calculated values from two methods (~2 kJ mol^{-1}). The average activation energy values of Ozawa and KAS methods for the 2nd step are 100.37 and 95.02 kJ mol^{-1}, respectively, which are close to each other (~5 kJ mol^{-1} difference). However, the higher activation energy values of the 2nd step compared to the 1st step in both methods can be interpreted that the dehydration in the 2nd step occurred in the long temperature range and completely dehydrated at elevated temperature (~700 °C).

Table 2 Activation energy values (E_α), pre-exponential factors (A), and correlation coefficients (r^2) calculated by using Ozawa and KAS methods for the 1st step of dehydration of $Mg_3(PO_4)_2{\cdot}8H_2O$

α	Ozawa method			KAS method		
	E_α/kJ mol^{-1}	A/min^{-1}	r^2	E_α/kJ mol^{-1}	A/min^{-1}	r^2
0.2	99.63±2.24	1.21×10^{12}	0.9990	98.03±2.38	6.73×10^{11}	0.9988
0.3	95.74±2.67	3.70×10^{11}	0.9984	93.83±2.81	1.84×10^{11}	0.9982
0.4	93.02±2.95	1.68×10^{11}	0.9980	90.88±3.10	7.67×10^{10}	0.9977
0.5	90.80±3.19	8.98×10^{10}	0.9975	88.48±3.36	3.82×10^{10}	0.9971
0.6	89.01±3.47	5.45×10^{10}	0.9970	86.52±3.66	2.18×10^{10}	0.9964
0.7	87.48±3.54	3.49×10^{10}	0.9967	84.84±3.74	1.31×10^{10}	0.9961
0.8	86.04±3.67	2.23×10^{10}	0.9963	83.23±3.87	7.88×10^{9}	0.9957
Average	91.67±3.10	2.78×10^{11}	0.9976	89.40±3.27	1.45×10^{11}	0.9972

Table 3 Activation energy values (E_α), pre-exponential factors (A), and correlation coefficients (r^2) calculated by using Ozawa and KAS methods for the 2nd step of dehydration of $Mg_3(PO_4)_2{\cdot}8H_2O$

α	Ozawa method		KAS method	
	E_α/kJ mol^{-1}	r^2	E_α/kJ mol^{-1}	r^2
0.2	76.64±10.25	0.9655	72.41±10.78	0.9575
0.3	77.73±9.67	0.9700	72.83±10.19	0.9623
0.4	89.23±7.72	0.9852	84.00±8.20	0.9813
0.5	98.74±12.36	0.9696	93.27±13.08	0.9621
0.6	105.85±17.24	0.9497	100.04±18.21	0.9378
0.7	120.74±19.66	0.9496	114.92±20.77	0.9387
0.8	133.68±20.78	0.9539	127.67±21.94	0.9442
Average	100.37±13.95	0.9634	95.02±14.74	0.9549

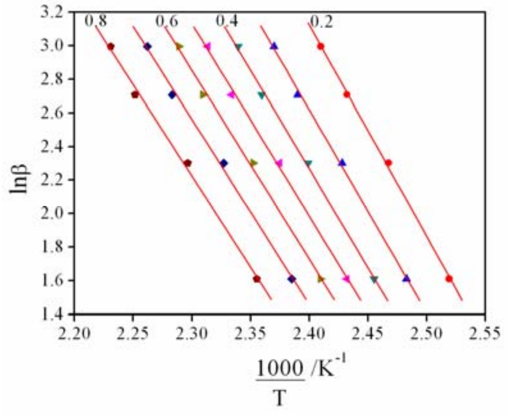

Figure 4 Ozawa plots for the 1st step of dehydration of $Mg_3(PO_4)_2{\cdot}8H_2O$

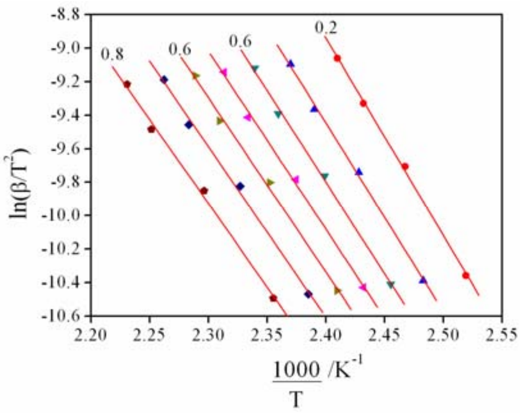

Figure 5 KAS plots for the 1st step of dehydration of $Mg_3(PO_4)_2{\cdot}8H_2O$

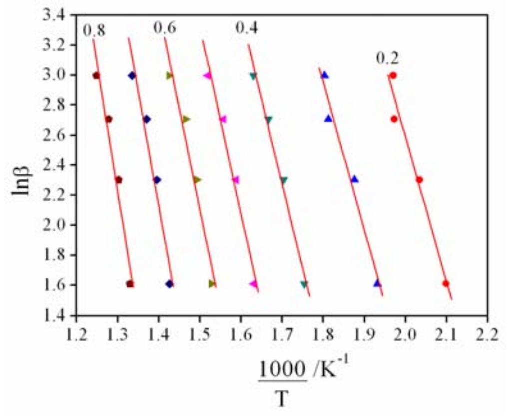

Figure 6 Ozawa plots for the 2nd step of dehydration of $Mg_3(PO_4)_2{\cdot}8H_2O$

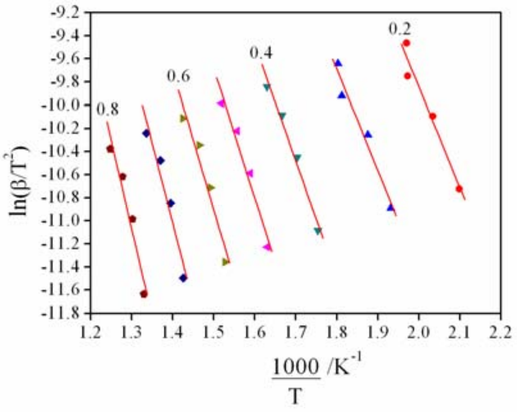

Figure 7 KAS plots for the 2nd step of dehydration of $Mg_3(PO_4)_2{\cdot}8H_2O$

According to Table 4, only the slopes determined from the function no. 11 are close to -0.1000 for two selected temperatures (150 and 155 °C) and the correlation coefficients are very close to each other. Hence, the most probable mechanism function for 1st step is in the integral form $g(\alpha) = -\ln(1-\alpha)$ and the differential form $f(\alpha) = (1-\alpha)$, which is the random nucleation and subsequence growth mechanism. This is a special case of Avrami–Erofeev model or the first order reaction (Khanwam & Flanagan 2006). The slopes determined from the function no. 6 is close to –1.0000 at 210 °C, while the slopes from the other functions are much deviated from unity (< –1.2000 and > –0.8000). The slopes determined for all functions at 220°C are not close to –1.0000 (< –1.2000 and > –0.8000). Thus, the most probable mechanism function for the 2nd step of dehydration cannot be one of the 26 types. Further study can be extended later. Subsequently, the pre-exponential factors of the 1st step can be particularly calculated from the intercept of the plots of Ozawa and KAS equations by inserting the most probable mechanism function $g(\alpha)$ and $f(\alpha)$ into the intercept of these plots. The obtained pre-exponential factors A of the 1st step from Ozawa and KAS calculations are 2.78×10^{11} and 1.45×10^{11}, respectively, as shown Table 2. These values from both methods agree well with each other.

Estimation of Thermodynamic Functions of the Transition State Complexes

The thermodynamic functions of the transition state complexes of the 1st step of dehydration calculated from Ozawa and KAS methods are summarized in Table 5. The negative values of $\Delta S^{\neq}$ from two methods reveal that the activated state is highly ordered compared to the initial state. These $\Delta S^{\neq}$ values suggest a large number of degrees of freedom due to the rotation and vibration which may be interpreted as a "slow stage". The positive values of $\Delta H^{\neq}$ agree well with the endothermic peaks in the DTA curves and notify that the dehydration is an endothermic process. The positivity of $\Delta G^{\neq}$ is controlled by a large amount of $\Delta H^{\neq}$ and a small of $\Delta S^{\neq}$ according to eq. (12). The positive values of $\Delta G^{\neq}$ at all methods can be interpreted that the dehydration process is not spontaneous.

Table 4 Most probable mechanism functions *g(α)*, slopes, and correlation coefficients of linear regression (r^2) at 150, 155, 210 and 220 °C

Temperature/°C	Mechanism no.	Slopes	r^2
150	6	-0.9693	0.9839
	11	*-0.9934*	*0.9957*
	26	-0.9874	0.9780
155	*11*	*-0.9387*	*0.9927*
	19	-1.0537	0.9699
	25	-0.9534	0.9677
210	6	-1.0364	0.9230
220	-	-	-

Table 5 $\Delta S^{\neq}$, $\Delta H^{\neq}$, and $\Delta G^{\neq}$ values for the 1st step of dehydration of $Mg_3(PO_4)_2 \cdot 8H_2O$

Thermodynamic functions	Ozawa	KAS
$\Delta S^{\neq}$/J K^{-1} mol^{-1}	-37.32	-42.74
$\Delta H^{\neq}$/kJ mol^{-1}	88.04	85.77
$\Delta G^{\neq}$/kJ mol^{-1}	104.35	104.44

Conclusions

The synthesized $Mg_3(PO_4)_2 \cdot 8H_2O$ dehydrates in two steps and its final dehydration product is found to be $Mg_3(PO_4)_2$. The TG/DTG/DTA curves demonstrated two dehydration steps. The kinetics of dehydration was carried out by using Ozawa and KAS equations. The activation energy values from both methods of the 1st step are very close to each other, while the activation energy values of the 2nd step are quite different. The mechanism of the 1st step of dehydration process is the first order reaction which the reaction rate is proportional to the concentration, amount or fraction remaining of reactant. In contrast, the most probable mechanism function of the 2nd step cannot be determined from the presented 26 reaction mechanism functions. The activation entropy ($\Delta S^{\neq}$), the activation enthalpy ($\Delta H^{\neq}$), and Gibbs free energy ($\Delta G^{\neq}$) changes of the transition state complexes of the 1st step from two methods can be calculated through the kinetic parameters. The values of $\Delta S^{\neq}$, $\Delta H^{\neq}$, and $\Delta G^{\neq}$ indicate the less disorder of transition state complex and the process is an endothermic as well as a non-spontaneous process.

Acknowledgement

We thank the Department of Chemistry and the Department of Physics (for XRD), Faculty of Science, Khon Kaen University for providing research facilities. The financial support from the Center of Excellence for Innovation in Chemistry (PERCH-CIC), Commission on Higher Education, Ministry of Education, is gratefully acknowledged.

References

Akahira, T. & Sunose, T. Res. Report Chiba Inst. Technol., 16, 22–31.

Aramendía, M.A., Borau, V., Jiménez, C., Marinas, J.M., & Romero, F.J. (1999). N-alkylation of aniline with methanol over magnesium phosphates. Appl. Catal. A: General, 183, 73–80.

Aramendía, M.A., Borau, V., Jiménez, C., Marinas, J.M., & Romero, F.J. (1999). Synthesis and characterization of magnesium phosphates and their catalytic properties in the conversion of 2-hexanol. J. Colloid Interface Sci., 217, 288–298.

Boonchom, B., & Danvirutai, C. (2009). Kinetics and thermodynamics of thermal decomposition of synthetic $AlPO_4 \cdot 2H_2O$. J Therm. Anal. Calorim., 98, 771–777.

Danvirutai, C., Noisong, P., & Youngme, S. (2010). Some thermodynamic functions and kinetics of thermal decomposition of $NH_4MnPO_4 \cdot H_2O$ in nitrogen atmosphere. J. Therm. Anal. Calorim., 100, 117–124.

Khanwam, A., & Flanagan, D. (2006). Solid-state kinetic models: Basics and mathematical fundamentals. J. Phys. Chem. B, 110, 17315–17328.

Kissinger, H.E. (1957). Reaction kinetics in differential thermal analysis. J. Anal. Chem., 29, 1702–1706.

Mesíková, Ž., Śulková, P., & Trojan, M. (2007). Synthesis and Characterization of newberyite. J. Therm. Anal. Calorim., 88(1), 103–106.

Noisong, P. & Danvirutai, C. (2010). Kinetics and mechanism of thermal dehydration of $KMnPO_4 \cdot H_2O$ in a nitrogen atmosphere. Ind. Eng. Chem. Res., 49, 3146–3151.

Noisong, P., Danvirutai, C., & Boonchom, B. (2009). Thermodynamic and kinetic properties of the formation of $Mn_2P_2O_7$ by thermal decomposition of $Mn(H_2PO_2)_2 \cdot H_2O$. J. Chem. Eng. Data, 54, 871–875.

Ozawa, T. (1965). A new method of analyzing thermogravimetric data. Bull. Chem. Soc. Jpn., 38, 1881–1886.

Rooney, J.J. (1995). Eyring transition-state theory and kinetics in catalysis. J. Mol. Catal. A: Chem., 96, L1–L3.

Senum, G.I. & Yang, RT. 1977. Rational approximations of the integral of the Arrhenius function. J. Therm. Anal. Calorim., 11, 445–447.

Sugiyama, S., Kondo, N., Satomi, K., Hayashi, H., & Moffat, J. (1995). Effect of tetrachloromethane as a gas-phase additive on the oxidative dehydrogenation of ethane over magnesium phosphate. J. Mol. Catal. A: Chem., 95, 35–43.

Tabtimsai, C. (2007). Raman and infrared spectroscopic studies of divalent cation phosphate hydrates related to saline soil. A thesis for the degree master of science in physical chemistry, Graduate School, Khon Kaen University.

Vlaev, L., Nedelchev, N., Gyurova, K., & Zagorcheva, M. (2008). A Comparative study of non-isothermal kinetics of decomposition of calcium oxalate monohydrate. J. Anal. Appl. Pyrol., 81, 253–262.

Vlase, T., Vlase, G., Doca, M., & Doca, N. (2003). Specificity of decomposition of solids in non-isothermal conditions. J. Therm. Anal. Calorim., 72, 597–604.